NEVIS - 9

NEVIS CYCLOTRON LABORATORIES

REACTIONS OF STOPPED π^- MESONS IN HYDROGEN AND DEUTERIUM

William Chinowsky

COLUMBIA UNIVERSITY
PHYSICS DEPARTMENT
Irvington-on-Hudson,
New York

Joint ONR - AEC Program
Office of Naval Research Contract
Contract N6-ori-110 Task No. 1

Nevis - 9
R - 104

Nevis Cyclotron Laboratories
Columbia University
Physics Department
Irvington-on-Hudson,
New York

REACTIONS OF STOPPED π^- MESONS IN HYDROGEN AND DEUTERIUM

William Chinowsky

CU-83-55-ONR-110-1-Physics

Submitted in partial fulfillment
of the requirements for the degree
of Doctor of Philosophy in the
Faculty of Pure Science, Columbia
University

April, 1955

Joint ONR-AEC Program
Office of Naval Research Contract
Contract N6-ori-110-Task No.1

REACTIONS OF STOPPED π^- MESONS IN HYDROGEN AND DEUTERIUM

I. INTRODUCTION:

A considerable quantity of information about the properties of the π meson has been derived from studies of slow π^- reactions in hydrogen and deuterium. The main features of the reactions were determined from the experiments of Panofsky, Aamodt and Hadley.[1] In these experiments, a target alternately filled with hydrogen and deuterium gases at a pressure of 3000 lb./sq.in., inside the cyclotron vacuum chamber, was exposed to secondaries produced at a beryllium target by 330 Mev protons. Measurements were made on the energy spectra of γ-rays produced in the two gases. The hydrogen spectrum showed two groups, one sharply peaked at 130 Mev, the lower rather broad near 70 Mev. It was concluded that the higher energy group results from the capture reaction:

$$\pi^- + P \rightarrow N + \gamma. \qquad (1)$$

This proof that radiative absorption takes place establishes with certainty that the π meson is a boson, a result for which there was already strong evidence from observation of π^- stars in photographic emulsions. From the observed energy of the γ-ray emitted in reaction (1), remembering that the π^- and proton interact essentially at rest, the mass of the π^- meson is determined

$$M_{\pi^-} = 275.2 \pm 2.5\ M_e.$$

A subsequent experiment by Crowe and Phillips,[2] using the same technique but with improved energy resolution has provided a precise measurement

$$M_{\pi^-} = 272.7 \pm 0.3\ M_e.$$

The low energy peak is presumed due to the reaction

$$\pi^- + P \rightarrow N + \pi^o,\ \pi^o \rightarrow 2\gamma. \qquad (2)$$

The γ-rays from the π^o decay are uniformly distributed in energy between the limits $M_{\pi^o}(1-\beta_o)\gamma/2$ and $M_{\pi^o}(1+\beta_o)\gamma/2$, where $\beta_o C$ is the velocity of the neutral meson, $\gamma = 1/\sqrt{1 - \beta_o^2}$. Analysis of the observed distribution in terms of the resolving power of the γ-ray detection system determines the limits of the distribution and leads to a value of the velocity of the π^o emitted in reaction (2). From this the difference in the masses of the charged and neutral meson was determined

$$M_{\pi^-} - M_{\pi^o} = 10.6 \pm 2.0\ M_e.$$

Further, the branching ratio between mesic and radiative absorption was determined by Panofsky et al,

$$\frac{R(\pi^- + P^- \rightarrow N + \pi^o)}{R(\pi^- + P \rightarrow N + \gamma)} = 0.94 \pm 0.20$$

The assumption that the low energy peak is due to the decay of neutral mesons produced by stopped negative mesons was verified in an experiment of Sachs and Steinberger.[3] Hydrogen was bombarded by a monoenergetic external meson beam and the two

γ-rays from the π^0 decay observed in coincidence.

Measurement of the γ-ray spectrum from deuterium disclosed a peak near 130 Mev, but an absence of γ-rays in the region near 70 Mev. The observed peak is attributed to the reaction

$$\pi^- + D \rightarrow 2N + \gamma. \qquad (3)$$

Comparison of the total yield of γ-rays from hydrogen and deuterium indicates that only 30 percent of the captures in deuterium are accounted for by the radiative capture reaction (3). It is inferred that 70 percent of the captures proceed through the reaction

$$\pi^- + D \rightarrow 2N, \qquad (4)$$

the neutrons were not observed directly.

As was first pointed out by Feretti,[4] this process provides a means of distinguishing between scalar and pseudoscalar π-mesons. The initial state for all capture reactions considered here is an S-state of the respective mesic atom. The π^--D system has positive or negative parity, depending on whether the π^- is scalar or pseudoscalar. Parity and angular momentum conservation require that the two neutron system have total angular momentum one, and the parity of the meson. A state of even parity and angular momentum one is forbidden to the two neutron system by the Pauli principle, and the two neutron absorption process is forbidden for scalar mesons. The argument is independent of the theoretical model for the process. If the reac-

tion is observed, then to rule out scalar parity for the pion it is only necessary to show that the reaction proceeds indeed from an S-state. Brueckner, Serber and Watson[5] have shown, using the measured cross section for the process $\pi^+ + D \rightarrow 2P$, extrapolated to lower energy, that capture from the excited states of the meson-deuteron atom does not compete favorably with electromagnetic deexcitation. At most one in thirty mesons is expected to be captured before reaching the ground state. Therefore, if more than one-thirtieth of the stopped mesons are captured according to process (4), the meson cannot be scalar. Since it has already been shown that the pion has zero spin,[6] the Panofsky result indicates that the π meson is pseudoscalar.

The branching ratio between mesic and radiative capture in deuterium was determined by Panofsky et al

$$\frac{R(\pi^- + D \rightarrow 2N + \pi^o)}{R(\pi^- + D \rightarrow 2N + \gamma)} = -0.003 \pm 0.073.$$

The rate for the process

$$\pi^- + D \rightarrow 2N + \pi^o \qquad (5)$$

compared to the rate for the corresponding process in hydrogen can provide evidence that the neutral pion is also pseudoscalar. If the π^- and π^o have the same parity, angular momentum and parity conservation, and the Pauli principle, require that the two neutron state be ^3P, and the π^o be in a P-state relative to the center of mass of the neutrons, whereas opposite parity for π^- and π^o would permit a ^1S two neutron state. Since the total energy available is only $\sim$1 Mev, and the overlap of P and S states is small, the reaction is highly forbidden if the π^- and π^o have the same parity. However, from considerations

of phase space alone, the π^o/γ branching ratio in deuterium is expected to be only $\sim$5 percent of that in hydrogen. The Panofsky result is not then of sufficient accuracy to decide whether a parity selection rule is required to explain the decreased rate for the absorption process $\pi^- + D \rightarrow 2N + \pi^o$.

In the series of experiments to be described here we have studied the capture reactions

$$\pi^- + P \rightarrow N + \pi^o, \quad \pi^o \rightarrow 2\gamma \qquad \text{(i)}$$

$$\pi^- + D \rightarrow 2N \qquad \text{(ii)}$$

$$\pi^- + D \rightarrow 2N + \pi^o, \quad \pi^o \rightarrow 2\gamma \qquad \text{(iii)}$$

in arrangements where the appropriate reaction products are detected in coincidence with incident negative mesons, some of which come to rest in liquid hydrogen or deuterium.

A measurement was made on the angular correlation of the two γ-rays emitted in reaction (i). This affords a measure of the π^o velocity, as did the energy distribution of Panofsky et al, and therefore a new measurement of the $\pi^- - \pi^o$ mass difference.

In view of the important consequences of the existence of the second reaction, we have performed an experiment to detect the two neutrons in coincidence. This provides a direct observation of the process and confirms the conclusions of Panofsky et al.

To determine more precisely the relative rate of reaction (iii), an attempt was made to detect, in coincidence, the two γ-rays from the neutral meson decay. The results indicate that the process is highly forbidden and give evidence for pseudoscalar parity of the neutral meson.

II. The Capture Process:

The process of slowing down and subsequent capture of π^- mesons in hydrogen has been discussed in detail by Wightman.[7] The sequence of events includes energy loss by the ordinary stopping power mechanism, further reduction in energy by collisions of the meson with orbital electrons of velocities comparable to that of the meson and subsequent capture in an outer orbit of a π^--proton atomic system. By collisions of the neutral system with hydrogen molecules energy is lost and the meson proceeds to the lowest state. Reduction of energy by radiative transitions is of less importance, in hydrogen, than collision processes. The total time for capture into a K shell, $\sim 10^{-9}$ sec., is small compared to the mean life for π-μ decay, $\sim 10^{-8}$ sec.[8] The capture process in deuterium is essentially the same as in hydrogen.

III. The Reaction $\pi^- + P \rightarrow N + \pi^o$, the π^--π^o Mass Difference:

A. Kinematics

1. Reaction Kinematics

The binding energy of the lowest state of the π^--proton atomic system, ~ 3 Kev, is negligible compared to the sensitivity of this experiment. The meson and proton are therefore considered to interact at rest. The process $\pi^- + P \rightarrow N + \pi^o$ then yields a neutron and neutral meson, the sum of whose kinetic energies is equal to the π^--π^o mass difference, minus the neutron-proton mass difference. From momentum and energy conservation,

$$\delta = M_{\pi^-} - M_{\pi^o} = \sqrt{(M_{\pi^-}{}^2 + M_p{}^2)\beta^2/(1-\beta^2) + M_N{}^2} - M_p/\sqrt{1-\beta^2} - M_{\pi^-}(1/\sqrt{1-\beta^2} - 1)$$

where βc is the velocity of the neutral meson. For small β

$$\delta \cong M_N - M_P + \beta^2 [M_{\pi^-} + M_{\pi^-}{}^2/M_N]/2$$

2. γ-γ Angular Correlation

In the π^o rest system the two decay γ-rays are emitted in opposite directions with equal energy. Let ξ be the angle between the direction of motion of one of the γ-rays in the rest system and the π^o velocity in the lab system. The angle ϕ between the two γ-rays in the lab system is then given by

$$\sin \phi/2 = (1-\beta^2)^{1/2}/[(1-\beta^2) \cos^2 \xi + \sin^2 \xi]^{1/2}$$

Considering the isotropy of the γ-ray distribution in the rest system, the probability of observing a pair of γ-rays with correlation angle between ϕ and $\phi + d\phi$ is

$$N(\phi) \sin \phi \, d\phi = \sin \xi \, d\xi = \frac{(1-\beta^2)^{1/2} \sin \phi \, d\phi}{(1-\cos \phi)^{3/2} \beta[(1-\cos \phi)/(1-\beta^2)-2]^{1/2}}$$

The correlation function for $\beta = 0.2$ is shown in Fig. 1. The smallest correlation angle at which γ-ray coincidences should be observed is

$$\phi_c = \cos^{-1} (2\beta^2 - 1)$$

For small velocities this cutoff angle is a linear function of β, with $\pi - \phi_c \cong 2\beta$. The error in β is therefore 1/2 the error ϵ_ϕ in the experimentally determined cutoff angle and the error in the mass difference will be approximately $1/2 \, M_{\pi^-} \beta \epsilon_\phi$.

B. Experimental Procedure

Negative mesons produced at the internal target of the

380 Mev Nevis Cyclotron are collimated in a channel of the 8' iron shielding wall and further sorted in momentum by a double-focusing magnet and the beam defining counters #1 and #2; see Fig.2. Counter #1 is a liquid scintillator 4-1/2 inches in diameter by 5/8 inch thick; counter #2 is a stilbene crystal 2-1/4 inches horizontally by 2-3/4 inches vertically by 1/8 inch in thickness. Between the two counters 5 gm/cm^2 of carbon and 5 gm/cm^2 of LiH are inserted. The absorber thickness is chosen to maximize the number of mesons which stop in the liquid hydrogen; the type of material to minimize coulomb scattering, consistent with convenience.

The liquid hydrogen target cup is a vertical cylinder, of .004 inches thick stainless steel, 3.1 inches in diameter and 4-1/2 inches high. The cup is soldered to a larger liquid hydrogen reservoir, which is surrounded by a liquid nitrogen jacket and the system is enclosed in a metal dewar. A thin wall (.006 inch Al foil) of the vacuum chamber exposes 3-3/4 inches, vertically, of the target cup.[9]

The γ-ray detectors, counters #3 and #4 are liquid scintillators 4 inches horizontally by 8 inches vertically by 1 inch in thickness, with the scintillating liquid viewed by 1P21 phototubes at each of the four corners. Before counters #3 and #4 are placed 3/8 inch thick lead converters. The centers of the γ-ray detection counters are each 27-1/2 inches from the center of the hydrogen well and are moved in the horizontal plane through the target center.

A block diagram of the electronics arrangement is shown in

Fig. 3. Signals taken in parallel from the phototubes of each counter are amplified in Hewlett Packard wide band amplifiers. Pairs of amplified signals are mixed in diode bridge coincidence circuits with resolving times of 10^{-8} sec. The coincidence pulses are amplified, discriminated in a diode circuit and shaped to give uniform output pulses 5 x 10^{-8} sec.long and of 15 volts amplitude.[10] The dead time of the pulse shaper is $\sim 10^{-7}$ sec. The monitor pulse 1-2 is scaled in a scale-of-four circuit having a dead time of 10^{-7} sec.[11] The 1-2 and 3-4 pulses are mixed again in a diode bridge coincidence circuit, amplified and taken in coincidence,in a circuit obtained from the Atomic Instrument Company, with the amplified 23 pulses. The final coincidence pulses 1234 + 23, and several intermediate coincidence rates are scaled in commercial scale-of-64 circuits.

To obtain the γ-γ coincidence rates we measure the four counting rates:

a) Pb converters in place, H_2 in target cup
b) Pb converters in place, target empty
c) Pb converters removed, H_2 in target
d) Pb converters removed, target empty

The γ-γ coincidence rate is then taken to be (a-b)-(c-d). The rates without converters were, however, so small that these runs were usually omitted.

C. Experimental Results

Preliminary measurements were made with counters #3 and #4 at 10 inches from the hydrogen well to determine the most advantageous absorber thickness between the beam defining counters.

The results are shown in Fig. 4. The measurements were not extended to larger and smaller absorber thicknesses since it has already been shown that such coincidences are due to stopped mesons.[3]

Table I shows four-fold coincidence rates as a function of the angle θ between the γ-ray detectors, each counter at a fixed distance of 27-1/2 inches from the hydrogen cup. Incident beam intensity in the 1,2 telescope was of the order of 2×10^5 counts per minute. Four-fold rates with hydrogen in the target cup varied from about 2 counts/min. at 165° to about .2 counts/min. at 145°. Background rates varied from approximately 1 percent of hydrogen events to ~50 percent at smaller angles. The data are presented in Fig. 7 in graphical form together with computed curves to be discussed below.

D. Resolution of Apparatus

Quantitative evaluation of the cutoff angle ϕ_c requires a knowledge of the resolution of the detection system. To this end consider counter #3 fixed and the hydrogen cylinder collapsed into a plane parallel to that of counter #3. Let $N(\phi)\sin\phi d\phi$ be the rate, per unit volume of well, of emission of γ-rays with correlation angle between ϕ and $\phi + d\phi$, and per unit solid angle of one γ-ray. The corresponding rate on the collapsed surface is then

$$\rho(x, y, \phi)dxdyd\phi = N(\phi) \sin \phi \, d\phi \sqrt{r^2 - x^2} \, dx \, dy$$

Here r is the well radius, x and y respectively the horizontal and vertical distances from the center of the well. Let x',y'

be the coordinates of a point on counter #3 and let a pair of γ-rays, γ_1 and γ_2 be emitted in dxdy, γ_1 striking counter #3 in dx'dy'. The rate for this process is $N(\phi) \sin \phi \, d\phi \sqrt{r^2-x^2}$ dxdy $\frac{dx'dy'}{2\pi R^2}$ where R is the radius of the right circular cylinder C, with axis coincident with the well axis, on which counters #3 and #4 move. Fig. 5 shows the geometrical details. The trajectories of γ_2 at the angle ϕ with γ_1 generate a cone of half angle $\Psi = \pi - \phi$ with axis along γ_1 projected back. Let x'',y'' be the point of intersection of the extension of γ_1 on C opposite counter #3. For small angles Ψ, the intersection of the cone and counter #4 may be approximated by the arc of a circle of radius $r = R \sin \Psi$ with the center at x'', y''. Note that $x' = 2x - x''$, $y' = 2y - y''$ and $dx'dy' = dx''dy''$. Further let $\ell(\phi, \theta, x'', y'')$ be the length of arc of the intersection of the γ_2 cone with counter #4, where θ is the angle between counters #3 and #4. The coincidence counting rate is then

$$C(\theta) = \int N(\phi) \sin \phi \, d\phi \iint \frac{dx''dy''}{2\pi R^2} \frac{\ell(\phi, \theta, x'', y'')}{2\pi R \sin \phi} \iint dxdy \sqrt{r^2-x^2} =$$

$$\int N(\phi) L(\theta, \phi) d\phi$$

where

$$L(\theta, \phi) = \iint \frac{dx''dy''}{(2\pi)^2 R^3} \ell(\phi, \theta, x'', y'') \iint dxdy \sqrt{r^2 - x^2}$$

is the resolution function. The x, y integral is elementary, the limits of integration are functions of x'', y''. The x'', y'' integral is approximated by a sum

$$L(\theta, \phi) \cong \sum_i F(x_i'', y_i'') \frac{\ell(\theta, \phi, x_i'', y_i'')}{(2\pi)^2 R^3} [\Delta x'' \Delta y'']_i$$

where $F(x_i'', y_i'') = \iint dxdy\sqrt{r^2-x^2}$. The regions in x'', y'' space are chosen so that $F(x_i'', y_i'')[\Delta x''\Delta y'']_i$ is a constant. The arc lengths ℓ_i are summed on a map measure fixed to a compass with the centers of the circles placed in the various regions of x'', y'' space. The resulting functions $L(\theta, \phi)$ for several values of θ are shown in Fig. 6.

E. The $\pi^- - \pi^o$ Mass Difference

The curves of counting rate vs angle shown in Fig. 7 were computed by performing, numerically, the integration

$$C(\theta) = \int_{\phi_1(\theta)}^{\phi_2(\theta)} L(\theta, \phi) \frac{(1-\beta^2)^{1/2} d\phi}{(1-\cos\phi)^{3/2}\, \beta[(1-\cos\phi)/(1-\beta^2)-2]^{1/2}}$$

for different values of β^2. Each curve is normalized to the same area as that of the experimentally determined curve. The experimental resolution is seen to be somewhat poorer than calculated. This may be, at least in part, due to scattering of the conversion electrons in the edges of the lead foil. The best fit is obtained with $\beta^2 = 0.040$ and the limits of β^2 are estimated to be 0.0365 and 0.0435. The mass difference is then

$$M_{\pi^-} - M_{\pi^o} = 8.8 \pm 0.6\ M_e$$

This is in good agreement with the earlier result of Panofsky, Aamodt and Hadley, $M_{\pi^-} - M_{\pi^o} = 10.6 \pm 2.0\ M_e$.

IV. The Process $\pi^- + D \rightarrow 2N$

A. Experimental Arrangement

The two neutrons, of ~68 Mev energy, emitted in the non-radiative capture reaction were detected using the arrangement

shown in Fig. 8. The incident beam is defined in momentum by the focussing magnet and counters #1 and #2, as discussed above, and degraded in energy in absorbers of 2 gm/cm^2 carbon, 5 gm/cm^2 LiH and 2.7 gm/cm^2 polyethylene.

The hydrogen target previously described[9] is used here with liquid deuterium in the well. The only modification required is the insertion of a plug to prevent communication between the hydrogen and deuterium reservoirs. The deuterium intake of the target is connected to the gaseous-deuterium filling system shown in Fig. 9. Before liquefaction the pressure of the gas in the 115 gallon reservoir is 21 lb/sq.in. On admission to the target the gas is cooled by passing successively through copper coils in the liquid nitrogen and hydrogen reservoirs. When equilibrium is reached, approximately 1/2 liter of liquid has accumulated and the pressure of the deuterium system is 5 lb/sq.in. The liquid deuterium in the reservoir can be admitted to the target cup and returned in the manner previously described. At the conclusion of the experiment the hydrogen is allowed to evaporate and the deuterium returns to the gas reservoir.

Counters #3 and #4, the neutron detectors, are liquid scintillators 2-1/2 inches in diameter and 2 inches thick along the direction of motion of the neutrons. The scintillating liquid is enclosed in a lucite cell, following a design of Garwin,[12] and is viewed by a single 5819 photomultiplier tube. Counters 5a, b, c and d are plastic scintillators 4-1/2 inches in diameter and 1/2 inch thick. The center of each neutron counter is

5-3/8 inches from the center of the target cup. The six counters of the detection system have a common axis passing through the center of the liquid deuterium cell.

The electronics arrangement is shown in Fig. 10. Signals from the counters 5a, b, c, and d are mixed in a circuit whose output is proportional to the sum of the inputs. An 'event' consists of a coincidence 1234 in anti-coincidence with the parallel connection of the set of four counters #5; the anti-coincidence circuit is a product of the Atomic Instrument Co. The neutrons are detected by means of stars or proton recoils made in counters #3 and #4. The discriminator on the 3-4 coincidence is adjusted so that pulses in #3 and #4 are rejected if the energy loss due to ionization is less than roughly 10 Mev. Charged particles are rejected in counters #5b and #5d. Low energy γ-rays converted in the neutron counters are rejected by the pulse height requirement and high energy γ-rays are rejected in counters #5a and #5c. The system is specific for the detection of N-N coincidences with neutron energy greater than $\sim$10 Mev.

The detection efficiency can be estimated from information on the N-P cross section[13] and star formation in carbon[14]. From the total N-P cross section at 68 Mev, assuming the angular distribution to be the same as at 90 Mev, we calculate the probability of producing recoil protons with energy greater than 10 Mev, and range insufficient to penetrate the rear anti-coincidence counter, $\epsilon_H = .02 \pm .004$. From the data of Kellogg, we estimate a cross section for star formation in carbon $\sim$200 mbn, giving the probability for creation of charged particles $\epsilon_C = .045 \pm .015$. Then the efficiency for 65 Mev neutron detection, with the arrangement shown is $\epsilon = .065 \pm .015$.

B. Experimental Results

1. The Process $\pi^- + D \rightarrow 2N + \gamma$

We have used the γ-rays of this reaction in order: (1) to determine the thickness of the absorber in the incident beam which maximizes the number of mesons which come to rest in the target and (2) to permit an estimate to be made of the ratio of the non-radiative to radiative capture rates $R = (\pi^- + D \rightarrow 2N)/(\pi^- + D \rightarrow 2N + \gamma)$. To detect the γ-rays counter #3 is replaced by an absorber, 1.8 gm/cm^2 polyethylene, with a converter of 7 gm/cm^2 lead directly in front of counter 5b. The circuits are arranged to record coincidences 12 and 125a5b. The product of solid angle and efficiency for this arrangement is $\epsilon_\gamma \Omega_\gamma = 0.2$. The 125a5b rate as a function of absorber thickness is shown in Fig. 11. The absorber used in the following experiments is 9.7 gm/cm^2. For this thickness the γ-ray counting rate is

$$CR_{2N+\gamma} = \frac{125a5b}{12} = (488 \pm 5) \times 10^{-6}$$

2. Determination of Discriminator Level

To set the discriminator on the 3-4 coincidence, counters 1, 3, 4, 2 are placed in the incident beam, and the 1234 coincidence rate measured as a function of the voltage on the phototubes of counters #3 and #4. The counting rate was measured with voltages of 1200^V, 1125^V, and 1050^V on the phototubes, so that the output pulse sizes were in the ratio 1:0.65:0.4. The energy distribution in the incident beam is peaked about 58 Mev, with full width at half-maximum $\sim$14 Mev; only mesons of energy

greater than 57 Mev are counted in this arrangement. The discriminator on the 3-4 coincidence is adjusted so that the 1234 rates, with the above phototube voltages, are in the ratio ~25:14:1, corresponding to that expected from the pulse height distribution deduced from the known energy distribution, if only pulses from mesons with ionization loss greater than ~10 Mev are registered in counters #3 and #4.

3. N-N Coincidences

The results of the search for neutron-neutron coincidences with the geometry of Fig. 8 and the electronics arrangement of Fig. 10 are given in Table II. The observed 2N rate is

$$CR_{2N} = \frac{(1234)5}{12} = (0.69 \pm 0.19) \times 10^{-6}$$

The branching ratio between non-radiative and radiative absorption is determined from the expression

$$R = \frac{CR_{2N}}{CR_{\gamma}} \frac{\epsilon\gamma}{(\epsilon_N)^2} \frac{\Omega\gamma/4\pi}{(\Omega_N/2\pi)g}$$

The quantity g is a geometrical factor; it is the probability that one of the two neutrons traverse counter #3 if it is known that the other has traversed counter #4 and that the two neutrons were emitted at 180^o to each other. Consider a small area ΔA on counter #3, collapsed into a plane. The probability of having a coincidence with one neutron striking ΔA is given by $\frac{1}{2\pi} \frac{\Delta A}{R^2} \Delta V/V$ where $\Delta V/V$ is the fraction of the total volume of the target cup included in a cone with apex in ΔA and base formed by counter #4, R is the average distance from ΔA to the target cup. The total probability is determined

by summing this quantity for various regions ΔA on counter #3, and g is computed to be 0.12. With the values $\epsilon_\gamma \Omega_\gamma = 0.2$, $\epsilon_N = 0.065 \pm 0.015$, $\Omega_N = 0.17$, we find $R = 1.5 \pm 0.8$. This is quite similar to the value $R = 2.4 \pm 0.5$ obtained by Panofsky et al from the comparison of γ-ray yields in hydrogen and deuterium. The discrepancy is within the experimental uncertainties.

4. N-N Angular Correlation

To test the identification of the observed events, we have measured the coincidence rate as a function of the angle subtended by the two neutron detectors at the target. This was, however, physically impossible with the arrangement of Fig. 8. It was necessary to sacrifice the anti-coincidence counters 5b and 5d to obtain the required mobility without reducing the counting rate to an impossible value. The new geometry is shown in Fig. 12. The additional absorber serves to make the system insensitive to low energy charged particles and the remaining anti-coincidence counters reject high energy γ-rays. The results are shown in Fig. 13. The theoretical curve represents the response of the detection system to particles emerging with equal probability from the various volume elements of the deuterium and at 180^o to each other. Computation of the variation of counting rate with angle proceeds similarly to that discussed above, with the counters at 180^o.

The consistency of the experimental points with the calculated function confirms the identification of the events as N-N coincidences.

V. The Reaction $\pi^- + D \rightarrow 2N + \pi^o$

A. Experimental Arrangement

The arrangement used to detect, in coincidence, the decay γ-rays from the π^o produced in this reaction is shown in Fig.14. The disposition of counters #1 and #2 and the absorbers in the incident beam is identical to that of Fig. 8 discussed in Section IIIA; counters 3,4,5 and 6 are plastic scintillators 4-1/2 inches in diameter and 1/2 inch thick, with counters #4 and #6 at 5-7/8 inches from the center of the target cup. Immediately before, and completely covering the area of counters #3 and #5 are lead converters of 1/4 inch thickness. The two counters of each telescope are separated by 3/4 inch thick polyethylene absorbers. The circuits are arranged to record coincidences between signals from 1-2, 3-4 and 5-6. These are then further mixed to yield coincidences 1234 and 123456, using electronic techniques similar to those previously discussed. The system is insensitive to low energy charged particles, in particular charged secondaries created in counters #3 and #5 by neutrons from the three capture reactions are of insufficient energy to traverse the polyethylene absorbers.

To determine the γ-γ coincidence rate, due to π^o decay γ-rays, and the single γ-ray rate, due primarily to γ-rays from the radiative capture reaction, the 1234 and 123456 rates are measured with the deuterium chamber filled and empty. As a check on the identification of the events with γ-rays, the rates are also measured with 3/8 inch aluminum replacing the 1/4 inch lead converters.

B. Experimental Results

The results of the search for π^o decay γ-rays are given in Table III. The rates with target filled and aluminum converter were approximately the same as the background rates with lead converter. We therefore take the difference of the rates with lead converter as the rate due to γ-rays from deuterium. These difference counts are given with their statistical errors. On the average, the incident beam intensity as measured in the 1-2 telescope was 3×10^5 counts per minute. The overall coincidence rate was $\sim$8 counts per hour with deuterium and the background $\sim$1/4 this value. A total of 23 overall coincidences was recorded with the cup filled.

As a check on the identification of these events with π^o decay γ-rays, the overall coincidence rate was measured with the two detecting telescopes subtending an angle of 140^o at the target. The rate decreased to 0.13 ± 0.07 per 10^6 monitor counts, indicating the particles observed in coincidence have correlation angles near 180^o.

C. Calculation of the Relative Rate

The branching ratio between neutral meson and γ-ray emission

$$R = (\pi^- + D \rightarrow 2N + \pi^o)/(\pi^- + D \rightarrow 2N + \gamma)$$

is calculated from the expression

$$R = \frac{CR_{\gamma\gamma}}{CR_\gamma} \frac{\epsilon_\gamma}{\epsilon_{\gamma\gamma}^2} \frac{G_\gamma}{G_D} - \frac{f_{\pi^o H}}{f_{\gamma D}} \frac{G_H}{G_D} N_H$$

where

$CR_{\gamma\gamma}$ = 123456 coincidence counting rate

CR_γ = 1234 single γ counting rate

ϵ_γ = efficiency for converting γ-rays from the reaction $\pi^- + D \rightarrow 2N + \gamma$

$\epsilon_{\gamma\gamma}$ = efficiency for converting decay γ-rays of the π^o produced in the reaction $\pi^- + D \rightarrow 2N + \pi^o$

N_H = fractional hydrogen impurity in the deuterium (a small hydrogen impurity contributes to the γ-γ rate via γ-rays from the decay of the π^o produced in the reaction $\pi^- + P \rightarrow N + \pi^o$)

f_{π^oH} = fractional rate for the mesic absorption process in hydrogen

$f_{\gamma D}$ = fractional rate for the radiative capture reaction in deuterium

G_γ = probability that single γ-rays emitted in deuterium will lie within the solid angle defined by counter #4; $G_\gamma = \Omega/4\pi$

G_D = geometrical factor giving the average probability that a π^o created within the deuterium cylinder will decay with γ-rays emitted in such direction that one traverses the 34 telescope, the other the 56 telescope

G_H = geometrical factor for decay γ-rays of the neutral mesons created in hydrogen.

An accurate calculation of the conversion efficiency is not possible because of the complications of multiple processes and scattering of the conversion electrons in the lead foil. Instead, we use the results of Cocconi and Silverman,[15] who measured the efficiency directly, using a similar geometry. They find the energy dependence can be represented by

$$\epsilon = .47\ [1 - e^{-(E-25)/40}],$$

with E the γ-ray energy in Mev. The spectrum of γ-rays from the process $\pi^- + D \rightarrow 2N + \gamma$ is sharply peaked at 129 Mev,[16]

the spectrum of γ-ray energies from decay of the maximum energy π^o produced in the mesic absorption process is flat between the limits 60 Mev and 76 Mev. The expression above then gives, for average energy γ-rays in each distribution $\epsilon_\gamma = 0.44$, $\epsilon_{\gamma\gamma} = 0.31$.

A mass spectrograph analysis of samples of deuterium removed from the gas-holder immediately after the run gave a value of the hydrogen impurity $N_H = .00523$[17]. The fractional rates f_{π^oH} and $f_{\gamma D}$ measured by Panofsky et al are $f_{\pi^oH} = .49 \pm .13$, $f_{\gamma D} = .29 \pm .04$

The factors G_D and G_H are determined from the geometry of the detection system and the angular correlation of the π^o decay γ-rays. Since it is expected that the energy distribution of the neutral mesons produced in the reaction $\pi^- + D \rightarrow 2N + \pi^o$ will be peaked near the maximum, because of the correlation in the direction of the two neutrons, we consider here only the γ-ray angular correlation for neutral mesons with this energy, velocity/C $\beta = 0.11$. The quantity G is given by $G_{\substack{H \\ D}} = \int P(\phi) N_{\substack{H \\ D}}(\phi) d\phi$ where $P(\phi)$ is the resolution function of the apparatus, $N_{\substack{H \\ D}}(\phi)$ is the correlation function for the decay γ-rays. Because of the symmetry of the arrangement here, we need consider only that 1/8 of the cup volume included between two perpendicular planes through the axis of the deuterium cylinder and a plane perpendicular to these and bisecting the axis. Further, consider this volume collapsed to a single point, $x = 0.62$, $y = 0.94$, $z = 0.62$ where the y axis is chosen along the cup axis, the origin of coordinates at the center of the cup. The probability of detecting a pair of γ-rays emitted from x, y, z with correlation angle ϕ is given by the expression, similar to

that obtained in the calculation of the angular resolution of the system used to detect γ-ray coincidences from hydrogen

$$P(\phi) = \iint \frac{dx'dy'}{2\pi R'^2} \frac{Z'}{R'} \frac{\ell(x',y',\phi)}{2\pi R''}$$

Here R' is the distance from x, y, z to the point x', y', z' on counter #4 and R'' is the distance from x, y, z to the point x'', y'', z'' on counter #6 intersected by the line joining x, y, z and x', y', z' (the direction of one γ-ray). This integral is calculated numerically, using the method discussed above. To find G_H and G_D, the integral $\int P(\phi)N_H^D(\phi)d\phi$ is evaluated numerically, yielding $G_H = .024$, $G_D = .028$. With these values we find the branching ratio

$$\frac{f_{\pi^o D}}{f_{\gamma D}} = -.0034 \pm .0043$$

Included in the error are the statistical uncertainties in the counting rates and the branching ratios measured by Panofsky, and estimates of errors ± 15 percent in ϵ_γ and $\epsilon_{\gamma\gamma}$, ± 10 percent in Ω and ± 25 percent in G_H and G_D.

The rate of the reaction $\pi^- + D \rightarrow 2N + \pi^o$ in deuterium is decreased relative to that of the corresponding reaction in hydrogen because of the decreased phase space available to the neutral meson. Only 1 Mev of kinetic energy of the reaction products is available. Consider then the reaction $\pi^- + D \rightarrow 2N + \pi^o$ in which the two neutrons are emitted in a ^1S state and neglect any dependence of the matrix element on angle or π^o momentum. The matrix element will be proportional to the N-N wave function evaluated for zero separation of the two neutrons. The

transition rate per unit π^o energy can then be written[18]

$$\frac{dT_{\pi^oD}}{dE_{\pi^o}} = \text{const} \times \Psi^2_{NN}(0) \times \frac{dN_{^1S}}{dE_{\pi^o}} \frac{P^2_{\pi^o}}{(2\pi\hbar)^3} \frac{dP_{\pi^o}}{dE} \times 4\pi$$

where $\frac{dN_{^1S}}{dE_{\pi^o}}$ is the number of ^1S states of the N-N system per unit π^o energy. Assuming a square well interaction of depth U and range r_o, the transition rate is

$$\frac{dT_{\pi^oD}}{dE_{\pi^o}} \propto \frac{\mu M^{3/2}}{8\pi^4\hbar^6} \sqrt{2\mu E_{\pi^o}} \frac{\sqrt{T_o - E_{\pi^o}\mu/\mu^*}[M(T_o - E_{\pi^o}\mu/\mu^*) + MU]}{M(T_o - E_{\pi^o}\mu/\mu^*) + MU \cos^2(\sqrt{T_o - E_{\pi^o}\mu/\mu^*}+U)Mr_o/\hbar c)}$$

where T_o is the available kinetic energy, M and μ the neutron and π^o masses, $\mu^* = 2M\mu/(2M + \mu)$, the reduced mass. Similar considerations for the reaction $\pi^- + D \rightarrow 2N + \gamma$ yield

$$\frac{dT_{\gamma D}}{dE_\gamma} \propto \frac{M^{3/2}}{8\pi^4\hbar^6} \times \frac{2\sqrt{T_\gamma - E_\gamma(1+E_\gamma/4M)}\ E_\gamma{}^2[M(T-E_\gamma[1+E_\gamma/4M]) + MU]}{M[T_\gamma - E_\gamma(1+E_\gamma/4M)]+MU \cos^2(\sqrt{M[T_\gamma - E_\gamma(1+E_\gamma/4M)+U]}r_o/\hbar c)}$$

here the available kinetic energy T_γ = 136 Mev. Taking U = 13 Mev, $r_o = 2.6 \times 10^{-13}$ cm. corresponding to the values deduced from low energy P-P scattering,[19] and numerically integrating the two energy distributions, we find $T_{\pi^oD}/T_{\gamma D} = C_{\pi^oD}/C_{\gamma D} \times .004$. The transition rates for π^- absorption leading to π^o or γ emission in hydrogen may be written

$$T_{\pi^oH} = C_{\pi^oH} \frac{P^2_{\pi^o}}{(2\pi\hbar)3} \frac{dP_{\pi^o}}{dE} 4\pi$$

$$T_{\gamma H} = C_{\gamma H} \frac{2P^2_\gamma}{(2\pi\hbar)3} \frac{dP_\gamma}{dE} 4\pi$$

where P_{π^o}, P_γ are the meson and γ-ray momenta respectively. The

constants will depend on the specific form of the interactions involved. In the ratio $\frac{T_{\pi^oD}}{T_{\gamma D}} / \frac{T_{\pi^oH}}{T_{\gamma H}}$, however, the constants should approximately cancel. The branching ratio between π^o and γ-emission from deuterium is then

$$\frac{R(\pi^- + D \rightarrow 2N + \pi^o)}{R(\pi^- + D \rightarrow 2N + \gamma)} = .004\left[P^2_{\pi^oH} \frac{dP_{\pi^oH}}{dE} / 2P^2_{\gamma H} \frac{dP_{\gamma H}}{dE}\right]^{-1} = \frac{0.004}{0.1} = .04$$

on the basis of phase space considerations only.

The branching ratio calculated from such phase space considerations is strongly dependent on the value of the $\pi^- - \pi^o$ mass difference. The error, ±7 percent, in the mass difference, leads to an uncertainty of ~±40 percent in the calculated rate for the reaction $\pi^- + D \rightarrow 2N + \pi^o$, ±5 percent in the rate for $\pi^- + P \rightarrow N + \pi^o$ and therefore ±35 percent in the branching ratio in deuterium. Then, with an error ±20 percent in the measured value of the branching ratio in hydrogen, the total error in the calculated deuterium branching ratio, due to the above uncertainties, is ±40 percent. Thus, in the absence of any parity selection rule, the branching ratio would be of the order of 5 percent. For pseudoscalar π^o, the two neutrons emitted in the reaction $\pi^- + D \rightarrow 2N + \pi^o$ are in P-states, and the matrix element will be greatly reduced. Meson-theoretic calculations by Tamor[20] show that the rate for emission of a pseudoscalar π^o is reduced by a factor of $\sim 10^{-3}$ relative to the rate for scalar π^o, The result obtained here, $f_{\pi^oD}/f_{\gamma D} < 0.1$ percent then is strong evidence for pseudoscalar π^o parity.

ACKNOWLEDGEMENTS

I should like to express my gratitude to Professor J. Steinberger for his continued efforts toward making a success both of the research described and of my graduate student career. Professor A. M. Sachs collaborated in the earlier phases of the experiments. Thanks are due also to the members of the operating crew and the secretarial staff of the Nevis Cyclotron Laboratories; and, more, to my wife, Joan, for her helpful cooperation.

REFERENCES

1. Panofsky, Aamodt and Hadley, Phys. Rev. 81, 565 (1951)
2. K. M. Crowe and R. H. Phillips, Phys. Rev. 96, 470 (1954)
3. A. Sachs and J. Steinberger, Phys. Rev. 82, 973 (1951)
4. B. Feretti, in Report of an International Conference on Low Temperatures and Fundamental Particles (The Physical Society London, 1946, Vol. 1, p. 75)
5. Brueckner, Serber and Watson, Phys. Rev. 81, 575 (1951)
6. Durbin, Loar and Steinberger, Phys. Rev. 83, 646 (1951); Clark, Roberts and Wilson, Phys. Rev. 83, 649 (1951)
7. A. S. Wightman, Phys. Rev. 77, 521 (1950)
8. Sargent, Rinehart and Lederman (private communication) have observed, in hydrogen gas at 18 atm. pressure, in a cloud chamber experiment, a ratio of π-μ decays to π^- stoppings <15 percent. In liquid hydrogen the ratio is then <1/2 percent.
9. Bodansky, Sachs and Steinberger, Phys. Rev. 93, 1367 (1954)
10. We are indebted to V. Fitch for the design of the circuit.
11. V. Fitch, Rev. Sci. Inst. 20, 942 (1949)
12. R. Garwin, Rev. Sci. Inst. 23, 755 (1952)
13. Hadley, Kelly, Leith, Segre, Wiegand and York, Phys. Rev. 75, 351 (1949)
14. D. A. Kellogg, Phys. Rev. 90, 224 (1953)
15. G. Cocconi and A. Silverman, Phys. Rev. 88, 1230 (1952)
16. R. H. Phillips and K. M. Crowe, Phys. Rev. 96, 484 (1954)
17. We wish to thank Mr. Harvey Goodspeed and the members of the staff of the Argonne National Laboratory who kindly performed the deuterium analyses.
18. cf the discussion of the reaction $P + P \rightarrow \pi^+ + N + P$ in: Fermi, Elementary Particles, Yale University Press, 1951
19. J. D. Jackson and J. M. Blatt, Rev. Mod. Phys. 22, 77 (1950)
20. S. Tamor, Phys. Rev. 82, 38 (1951)

FIGURE CAPTIONS

FIGURE

1. Correlation function for γ-rays from decay of neutral mesons with velocity/c, $\beta = 0.2$.

2. Experimental arrangement to measure γ-γ angular correlation.

3. Electronics arrangement used in detection of decay γ-rays of the π^o produced in the reaction $\pi^- + P \rightarrow N + \pi^o$.

4. Variation of γ-γ counting rate with thickness of the absorber in the incident beam.

5. Geometry for calculation of the angular resolution of the π^o decay γ-ray detection system.

6. Resolution functions of the γ-γ detecting system.

7. γ-γ coincidence rate vs. angle between detecting counters. Solid curves are calculated.

8. Experimental arrangement to detect coincidences between neutrons from the reaction $\pi^- + D \rightarrow 2N$.

9. Gaseous-deuterium filling system.

10. Electronics arrangement used for detection of N-N coincidences.

11. Counting rate of γ-rays from the reaction $\pi^- + D \rightarrow 2N + \gamma$ vs. thickness of absorber in the incident beam.

12. Experimental geometry used to measure N-N coincidence rate as a function of the angle θ between the neutron detectors.

13. Observed and calculated N-N coincidence counting rates vs. the angle subtended by the neutron detectors at the deuterium target.

14. Experimental arrangement used in measuring γ-γ rates from the reaction $\pi^- + D \rightarrow 2N + \pi^o$, $\pi^o \rightarrow 2\gamma$, and single γ-rays from $\pi^- + D \rightarrow 2N + \gamma$.

TABLE I

Experimental Results; Variation of Four-Fold Coincidence Rates with θ, the Angle between γ-ray Detectors. Counts are per 2.048×10^6 Monitor Counts.

θ	Number Counts Hydrogen In Cup	Number Counts Without Hydrogen	Net Due To Hydrogen
180^o	22.2 ± 1.5	1.3 ± 0.5	20.9 ± 1.6
170^o	21.6 ± 1.5	1.3 ± 0.7	20.3 ± 1.7
165^o	24.6 ± 1.9	1.0 ± 1.0	23.6 ± 2.1
160^o	22.4 ± 1.4	0.9 ± 0.9	21.3 ± 1.7
155^o	12.8 ± 1.2	0.7 ± 0.5	12.1 ± 1.3
150^o	6.5 ± 0.8	0.8 ± 0.6	5.7 ± 1.0
145^o	2.3 ± 0.5	1.4 ± 0.5	0.9 ± 0.7

TABLE II

N-N Coincidences observed with Geometry of Fig. 8. Rates are per 10^6 Incident Mesons as Measured in 12 Coincidence

	Counts With D_2 in Cup	Counts With Cup Empty	Net Due to D_2
1234	1.02 ± 0.19	0.08 ± 0.1	0.94 ± 0.20
1234-5	0.70 ± 0.16	0.08 ± 0.1	0.62 ± 0.19

TABLE III

γ-γ Coincidence and Single γ-ray Rates from Deuterium. Rates are per 10^6 Incident Mesons as Measured in 12 Coincidence

Converter	Counts with D_2		Counts without D_2		Net due to D_2	
	1234	1234-56	1234	1234-56	1234	1234-56
1/4'' Pb	759±4	.48±.09	271±3	.12±.06	488±5	.36±.11
3/8'' Al	308±3	.07±.05				

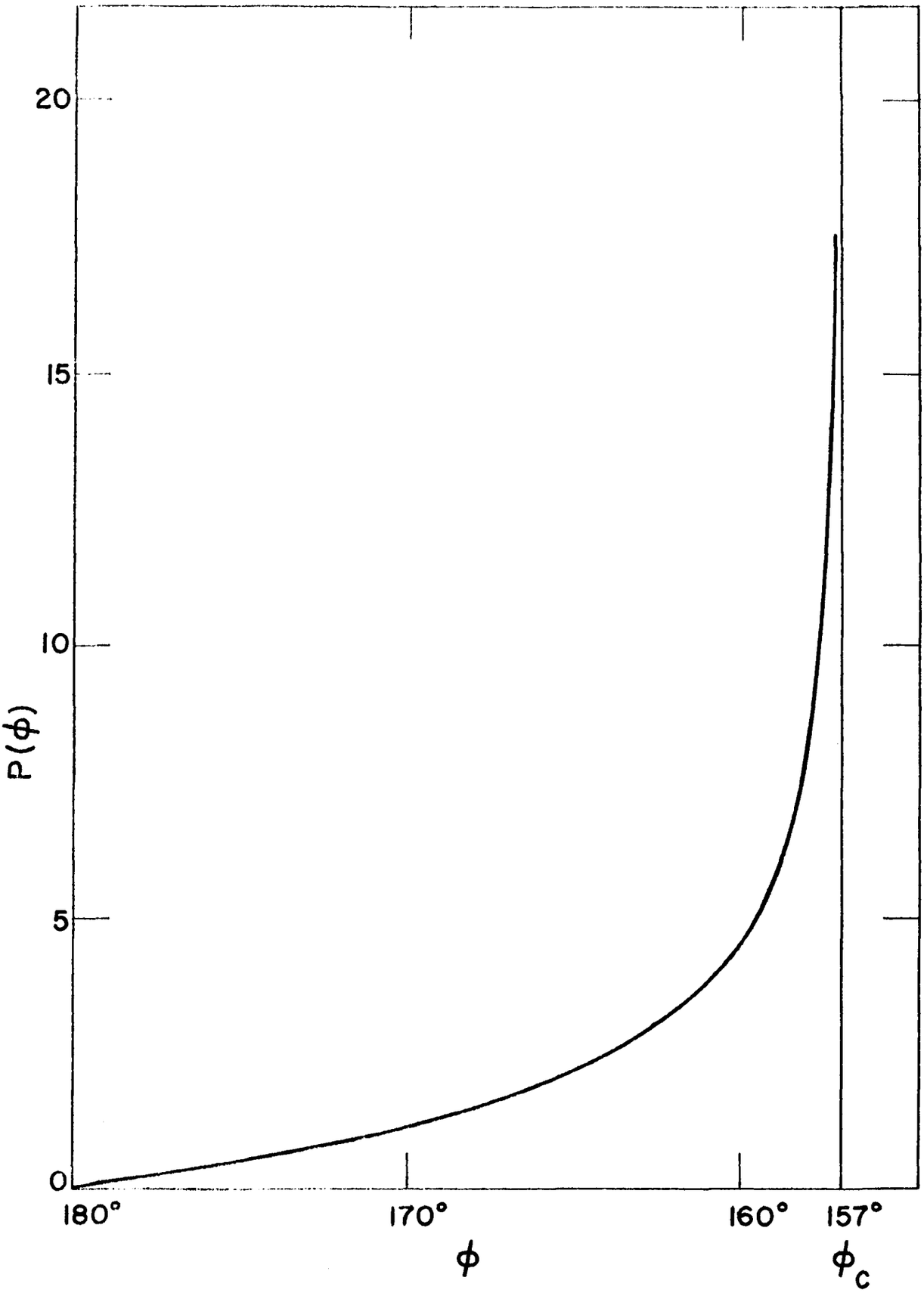

FIG. 1

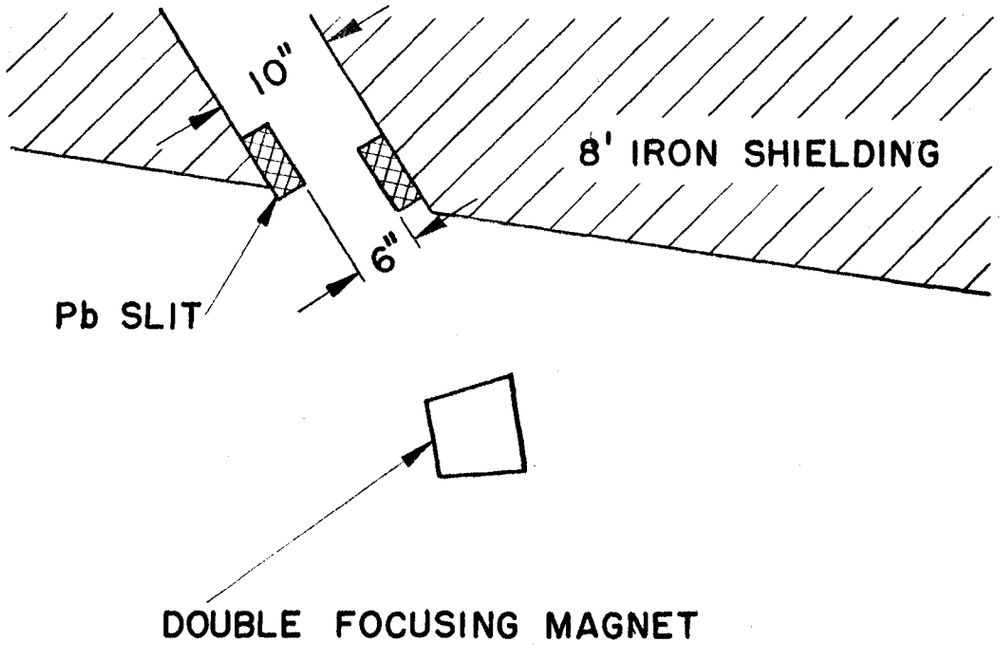
10"
8' IRON SHIELDING
6"
Pb SLIT
DOUBLE FOCUSING MAGNET

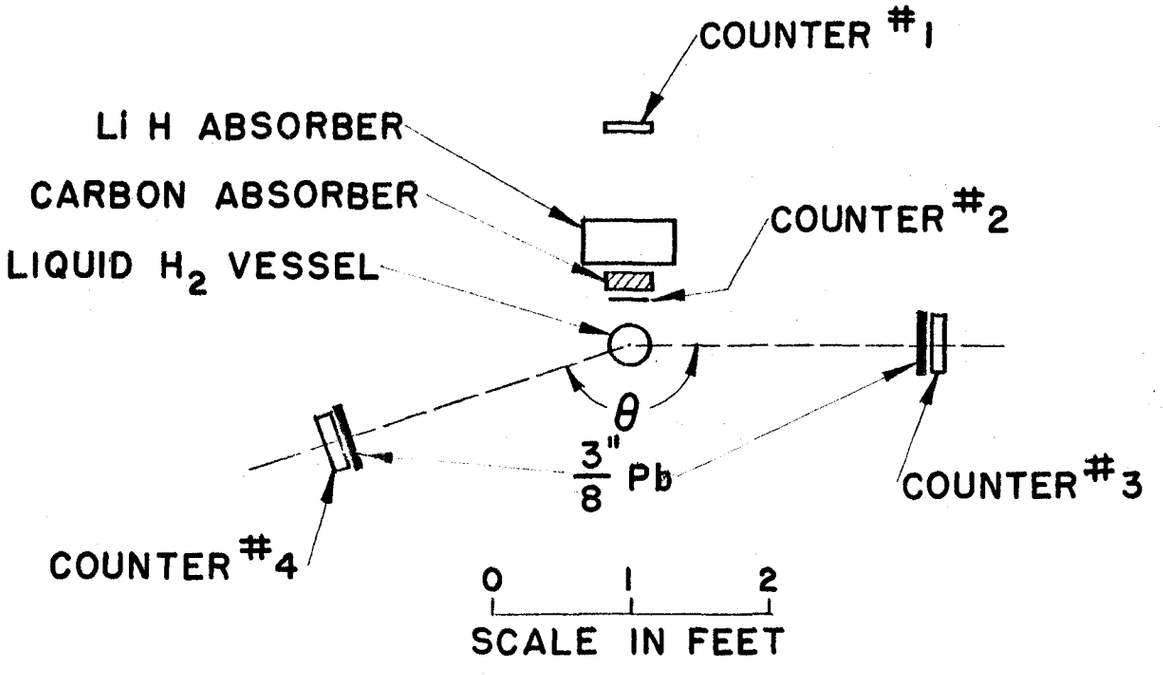
COUNTER #1
LiH ABSORBER
CARBON ABSORBER
LIQUID H_2 VESSEL
COUNTER #2
θ
3/8" Pb
COUNTER #3
COUNTER #4
0 1 2
SCALE IN FEET

FIG. 2

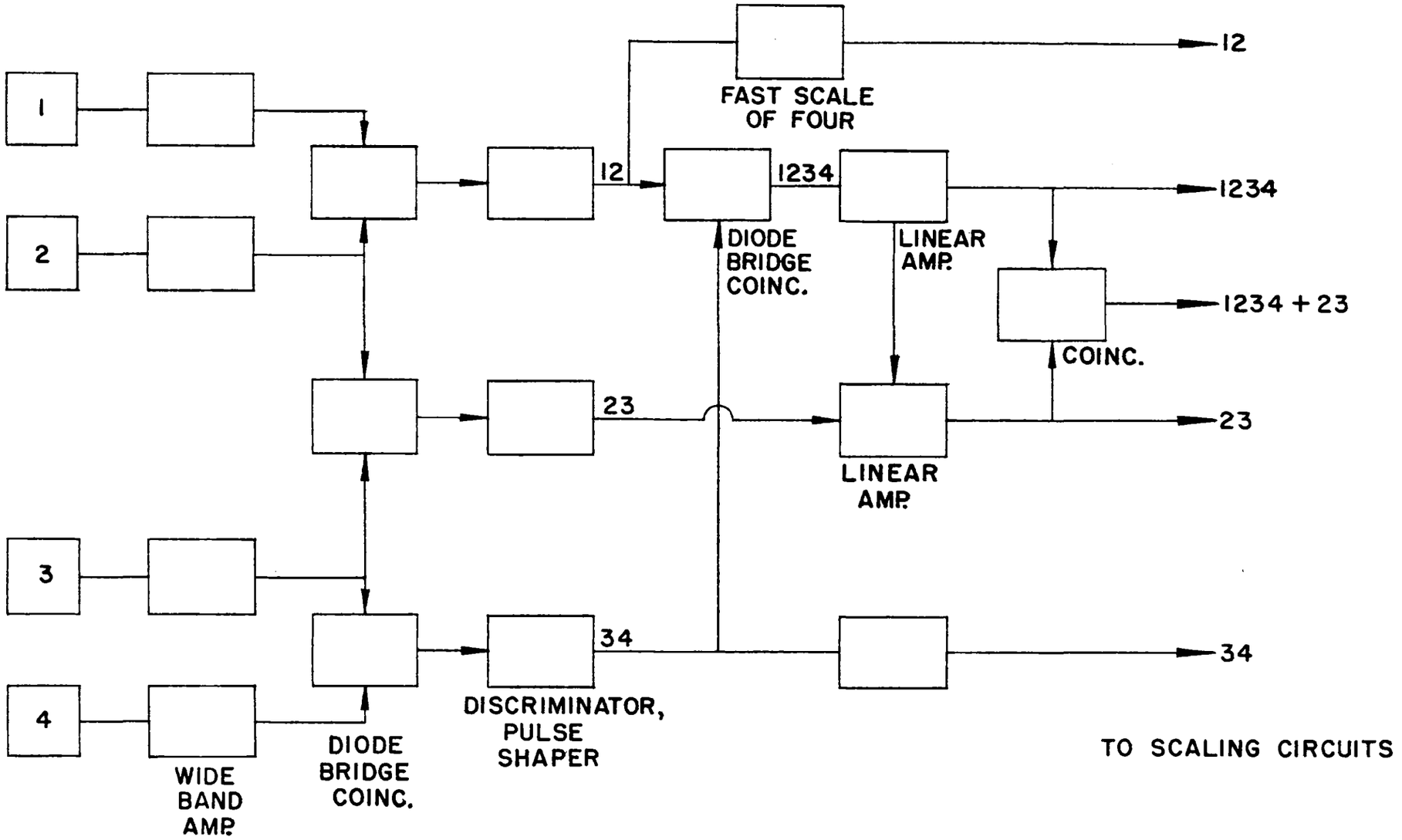
1
2
3
4
12
23
34
1234
1234 + 23
FAST SCALE OF FOUR
DIODE BRIDGE COINC.
LINEAR AMP.
COINC.
LINEAR AMP.
WIDE BAND AMP.
DIODE BRIDGE COINC.
DISCRIMINATOR, PULSE SHAPER
TO SCALING CIRCUITS

FIG.3

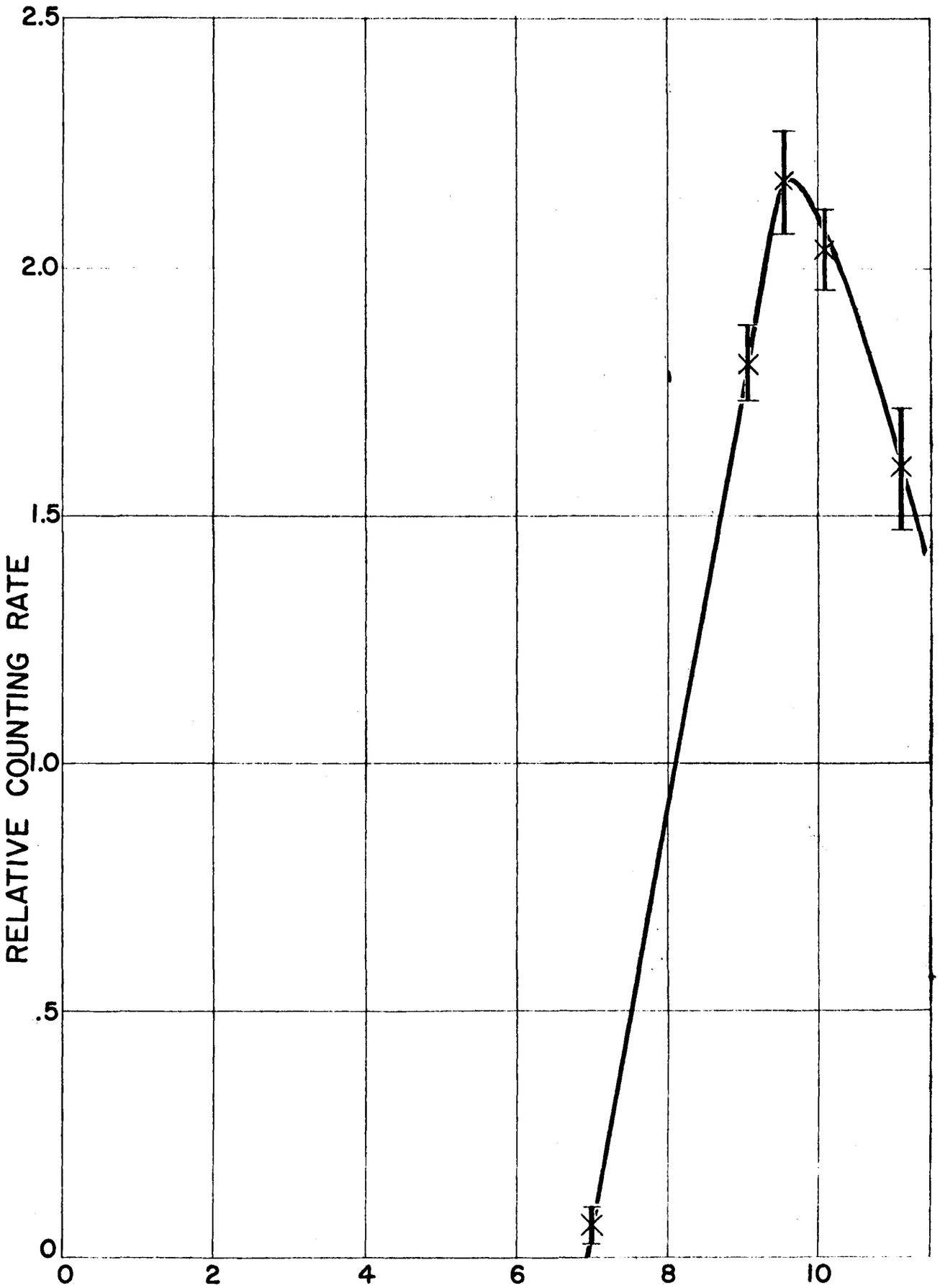
2.5
2.0
1.5
1.0
.5
0
RELATIVE COUNTING RATE
0
2
4
6
8
10
ABSORBER THICKNESS IN GM/CM^2 CARBON EQUIV.

FIG. 4

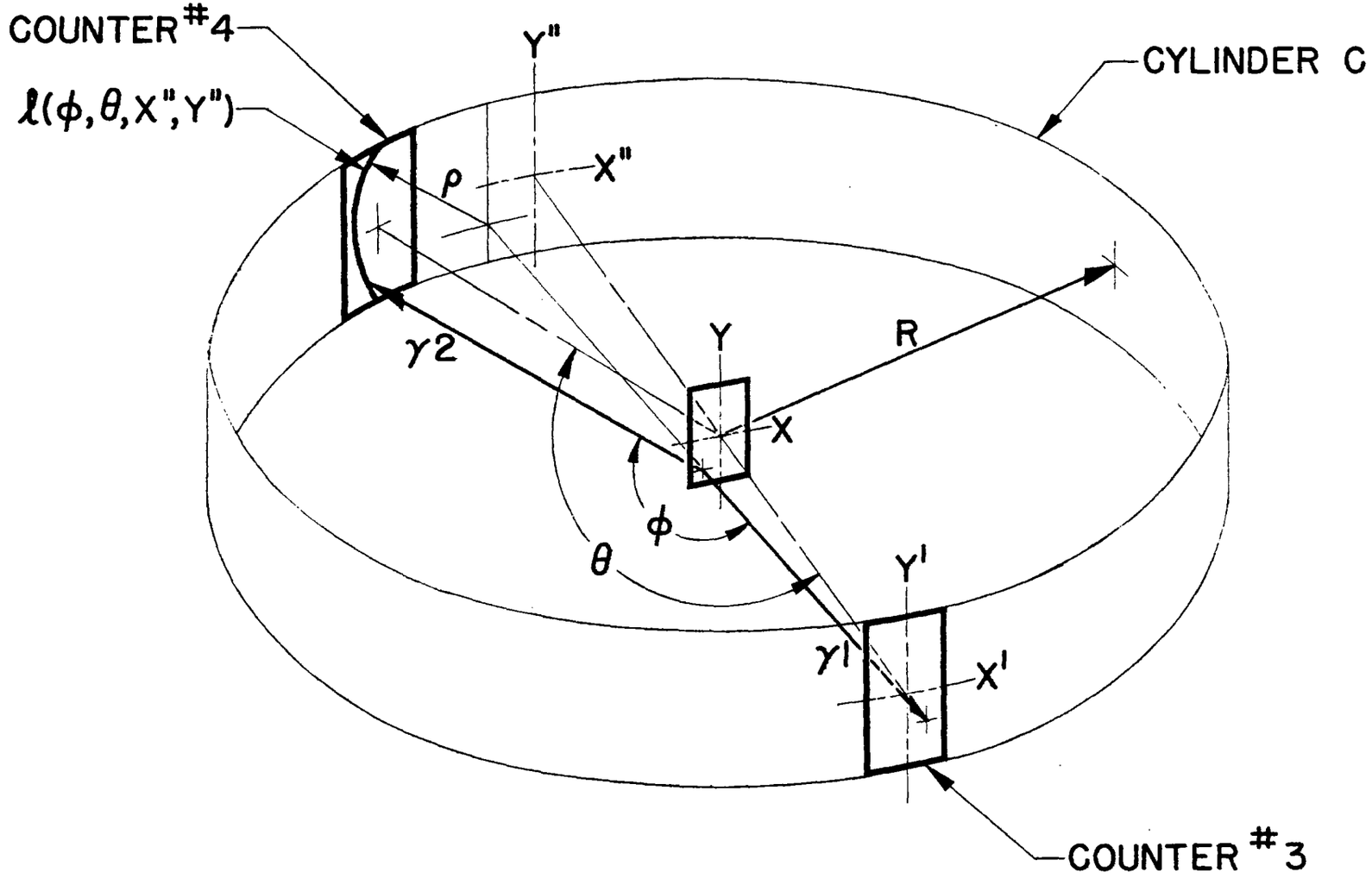
COUNTER #4
$\ell(\phi,\theta,X'',Y'')$
Y"
CYLINDER C
ρ
X"
γ2
Y
R
X
φ
θ
Y'
γ1
X'
COUNTER #3

FIG. 5

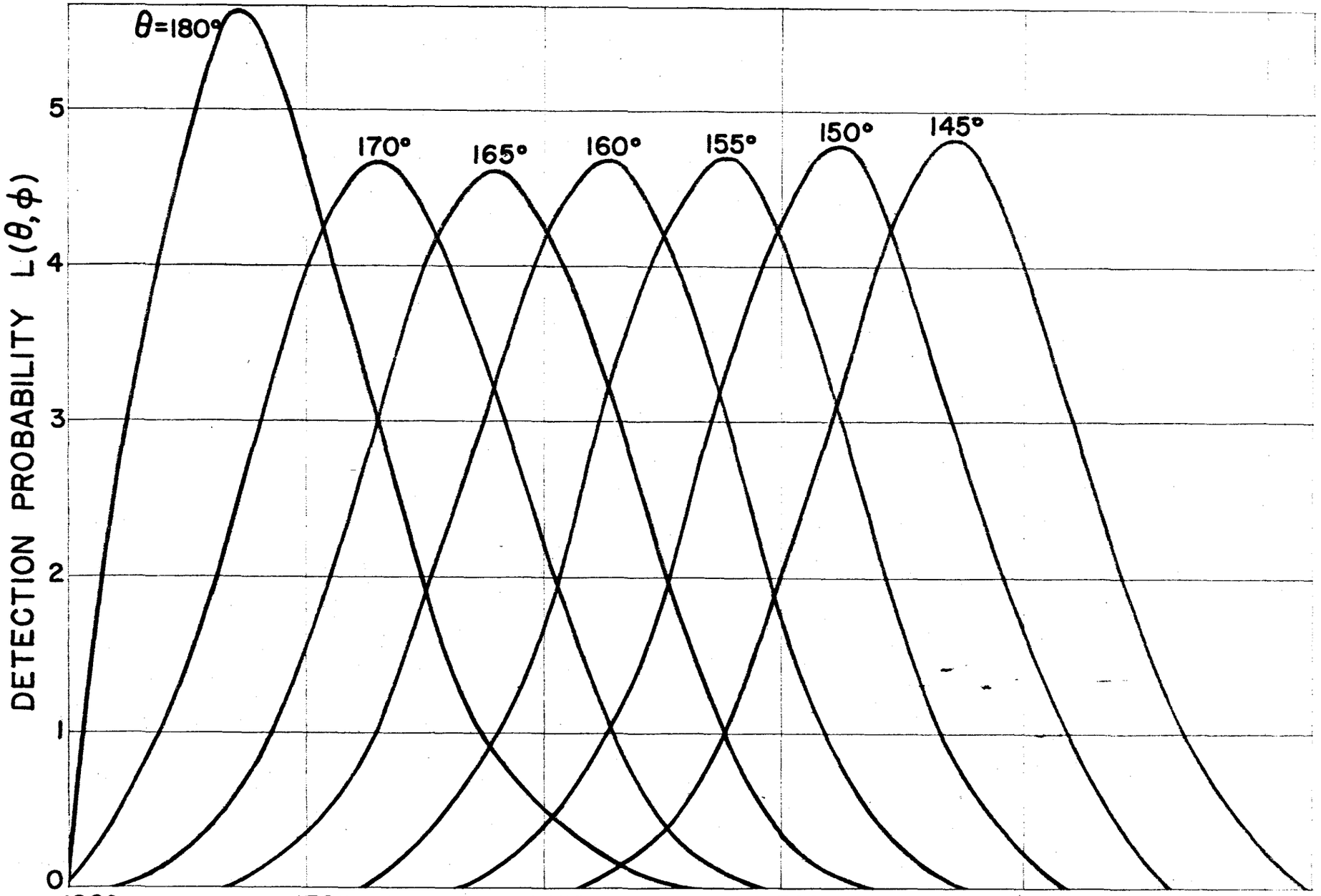
θ=180°
170°
165°
160°
155°
150°
145°
DETECTION PROBABILITY L(θ,φ)
0
1
2
3
4
5
180°
170°
160°
150°
140°
130°
CORRELATION ANGLE φ

FIG.6

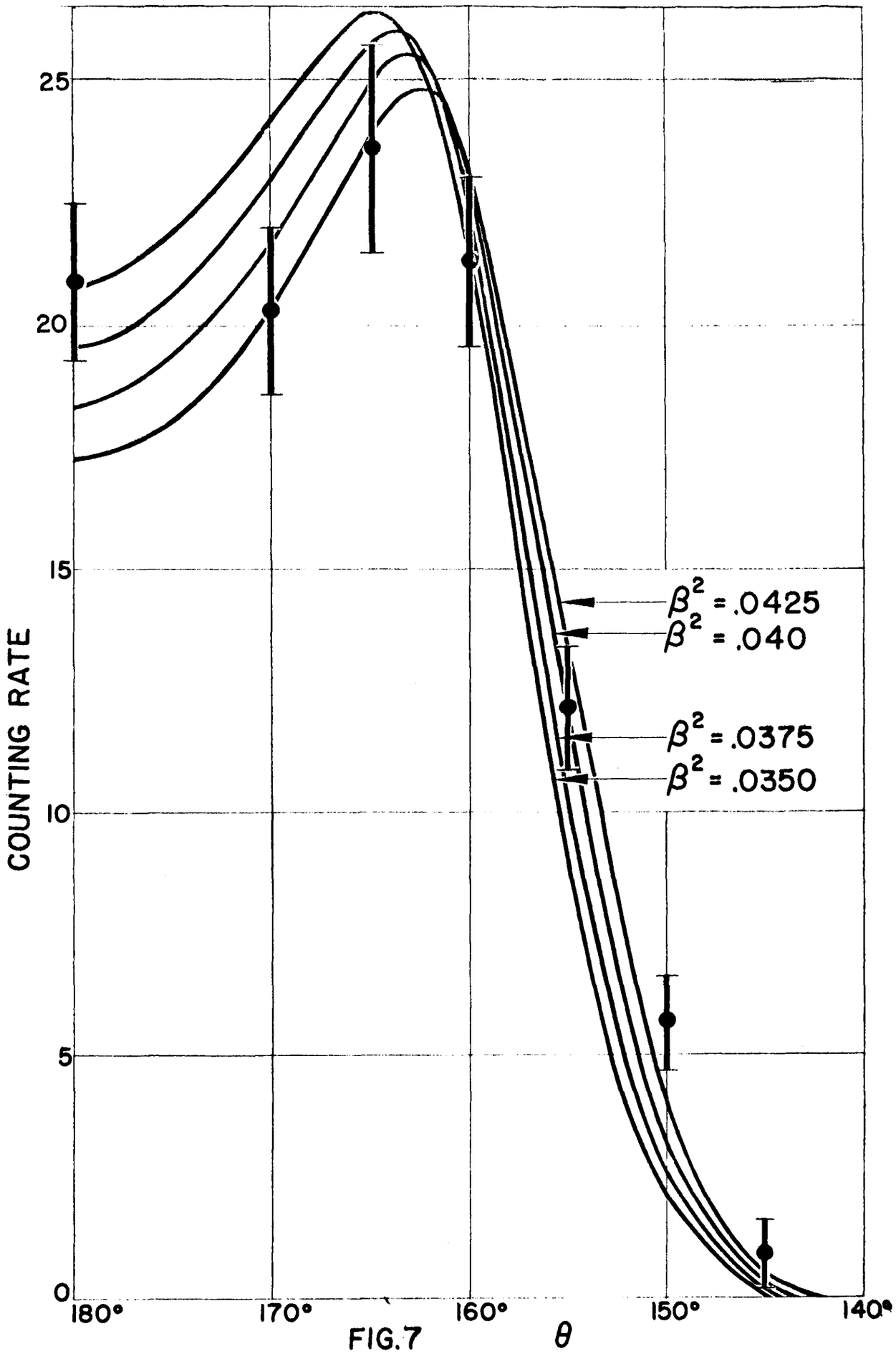
25
20
15
10
5
0
COUNTING RATE
$\beta^2 = .0425$
$\beta^2 = .040$
$\beta^2 = .0375$
$\beta^2 = .0350$
180°
170°
160°
150°
140°
θ

FIG. 7

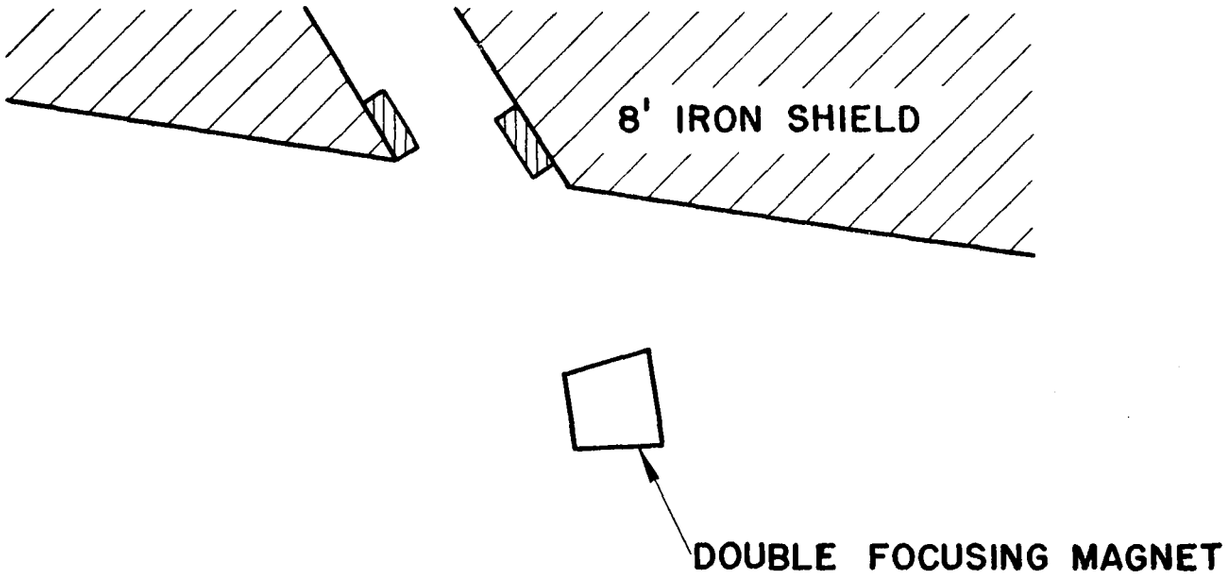
8' IRON SHIELD
DOUBLE FOCUSING MAGNET

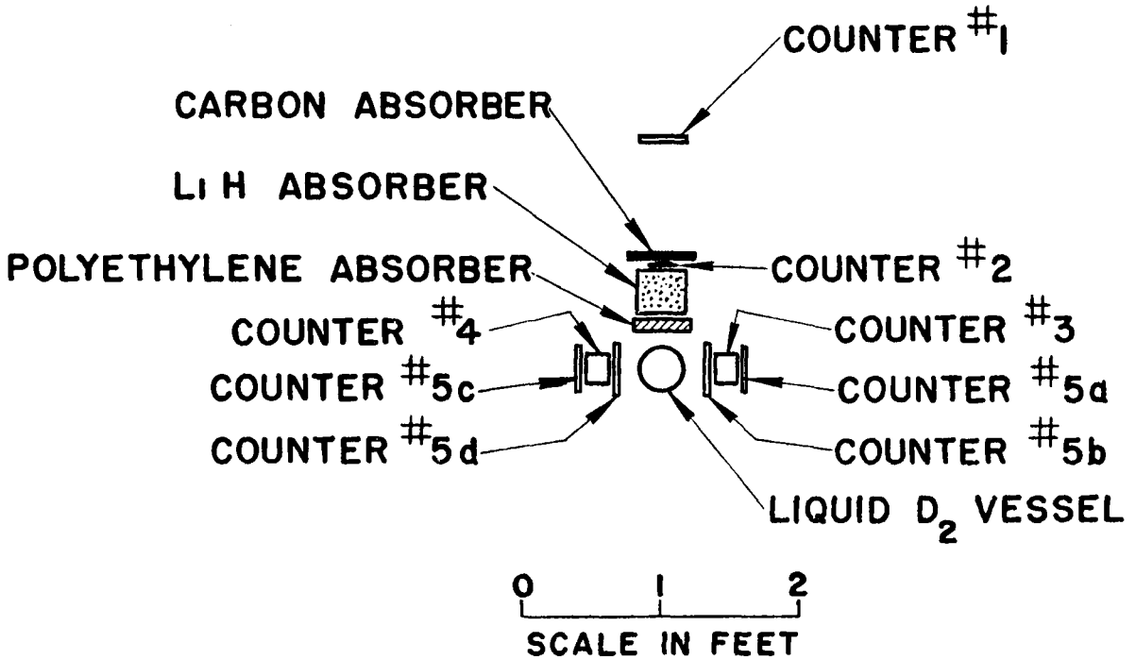
COUNTER #1
CARBON ABSORBER
Li H ABSORBER
POLYETHYLENE ABSORBER
COUNTER #2
COUNTER #4
COUNTER #3
COUNTER #5c
COUNTER #5a
COUNTER #5d
COUNTER #5b
LIQUID D2 VESSEL
0
1
2
SCALE IN FEET

FIG.8

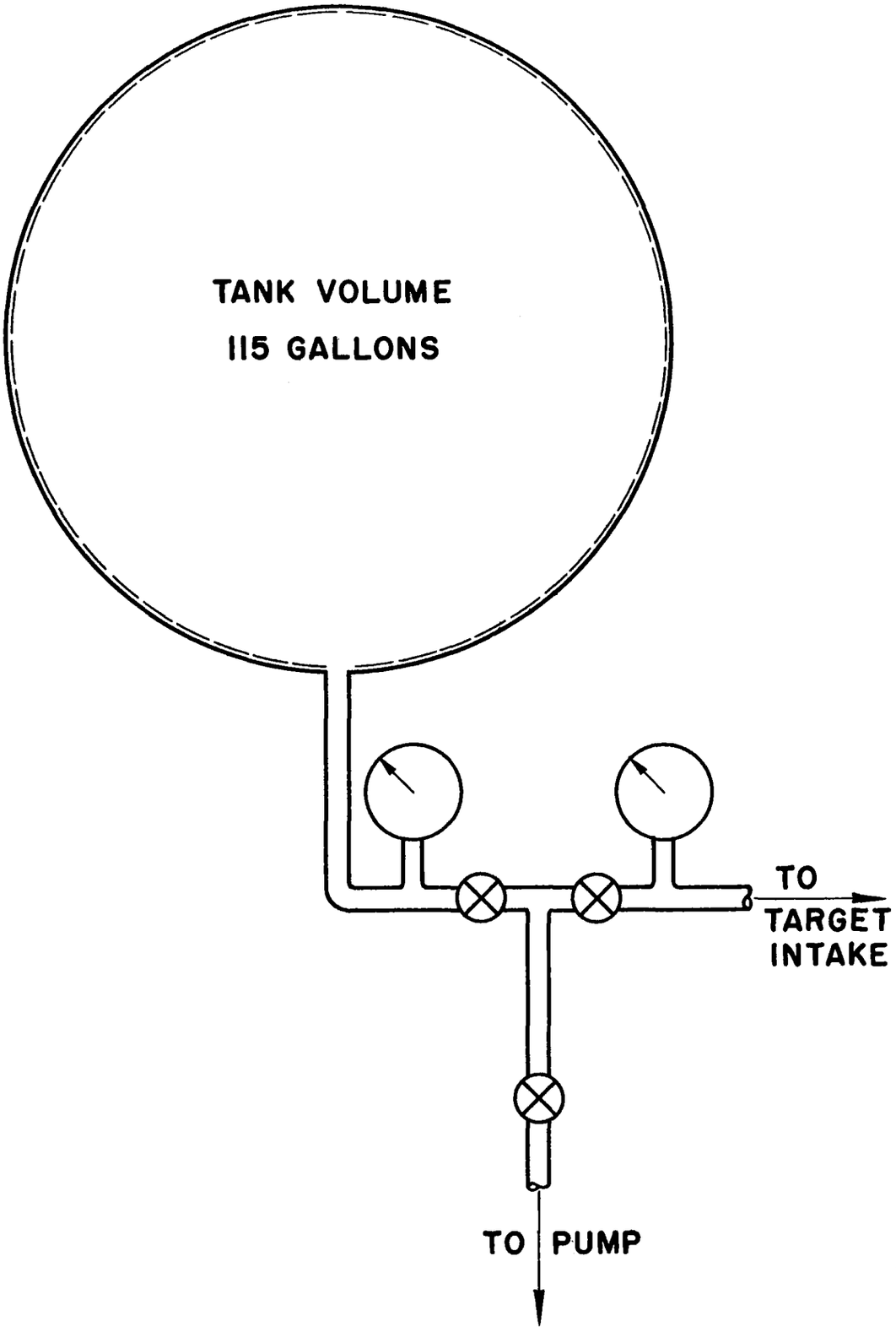

FIG.9

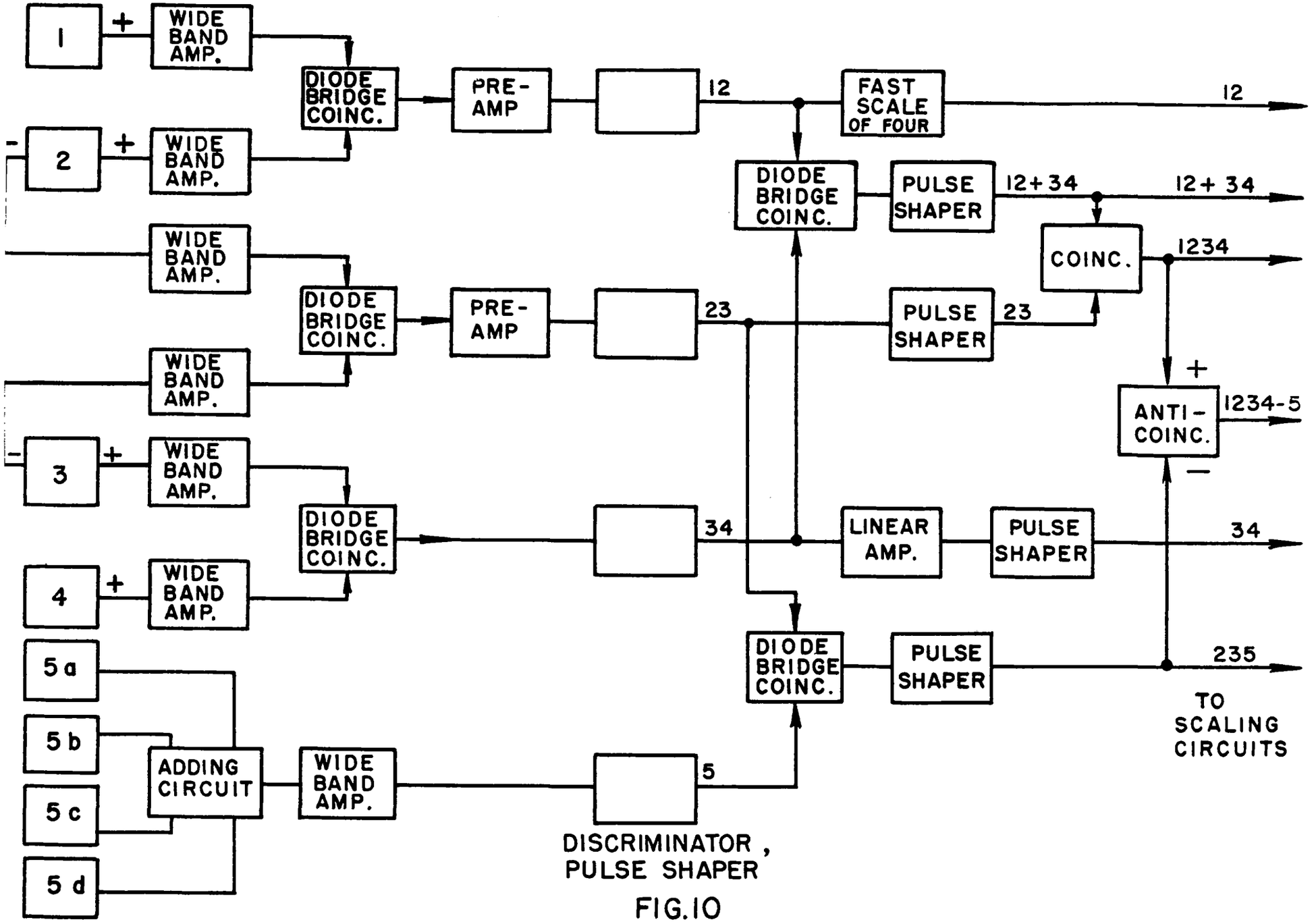
1
+
WIDE BAND AMP.
DIODE BRIDGE COINC.
PRE-AMP
12
FAST SCALE OF FOUR
12
-
2
+
WIDE BAND AMP.
DIODE BRIDGE COINC.
PULSE SHAPER
12+34
12+34
WIDE BAND AMP.
COINC.
1234
DIODE BRIDGE COINC.
PRE-AMP
23
PULSE SHAPER
23
WIDE BAND AMP.
+
ANTI-COINC.
1234-5
-
3
+
WIDE BAND AMP.
DIODE BRIDGE COINC.
34
LINEAR AMP.
PULSE SHAPER
34
4
+
WIDE BAND AMP.
DIODE BRIDGE COINC.
PULSE SHAPER
235
5a
5b
5c
5d
ADDING CIRCUIT
WIDE BAND AMP.
5
TO SCALING CIRCUITS
DISCRIMINATOR, PULSE SHAPER

FIG.10

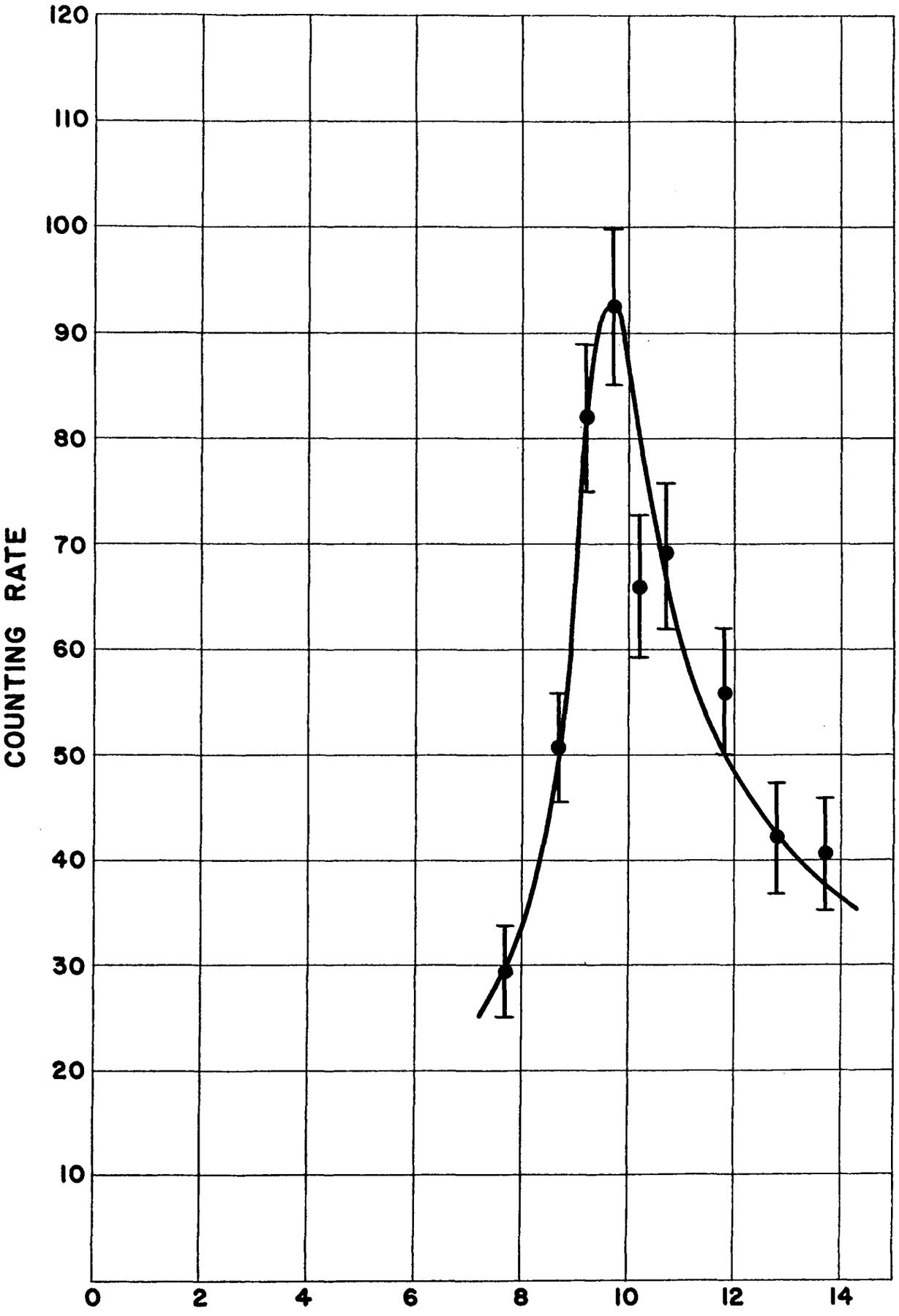
120
110
100
90
80
70
60
50
40
30
20
10
COUNTING RATE
0
2
4
6
8
10
12
14
ABSORBER THICKNESS (GM/CM 2 CARBON EQUIV.)

FIG. 11

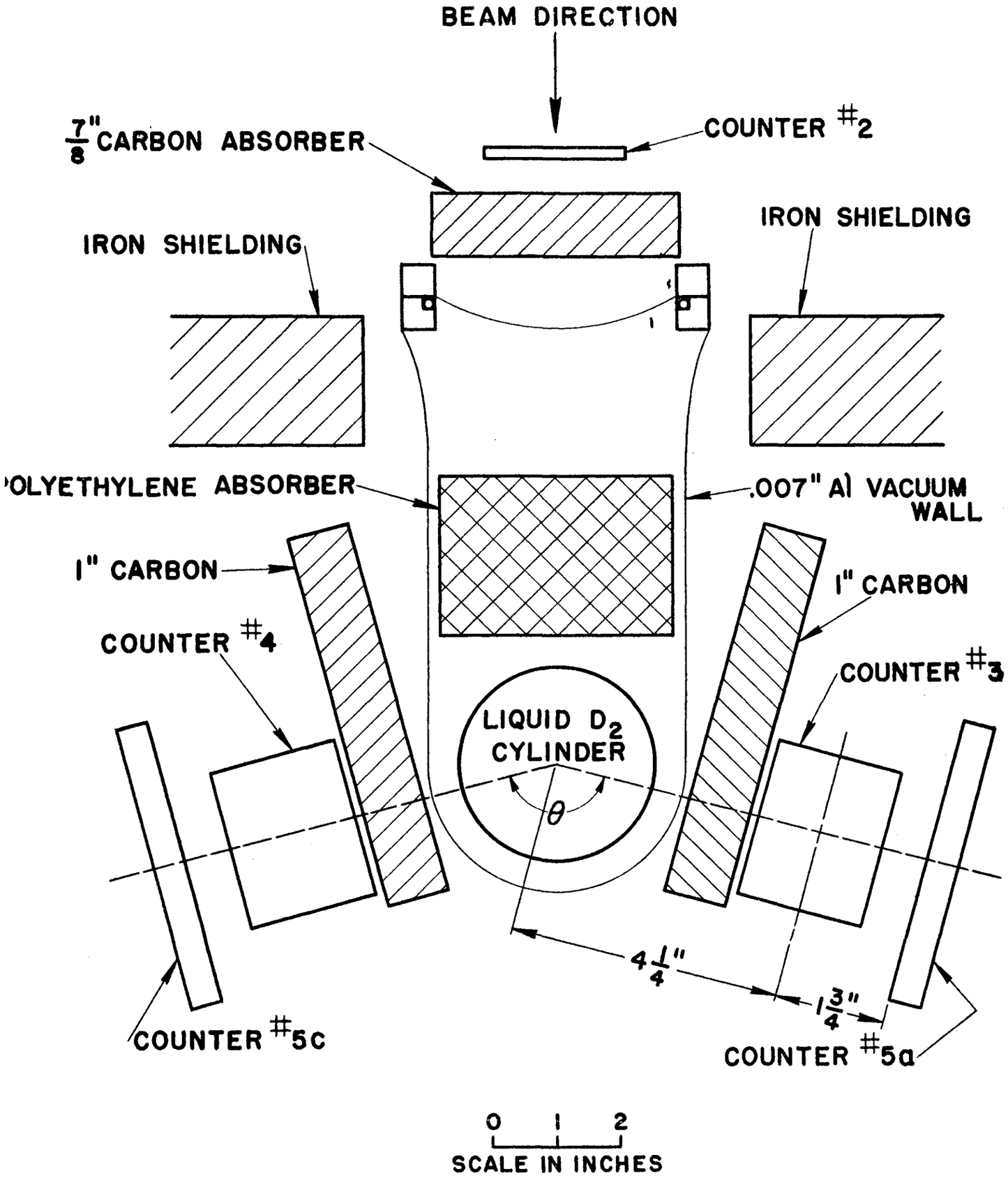
BEAM DIRECTION
7/8" CARBON ABSORBER
COUNTER #2
IRON SHIELDING
IRON SHIELDING
POLYETHYLENE ABSORBER
.007" Al VACUUM WALL
1" CARBON
1" CARBON
COUNTER #4
COUNTER #3
LIQUID D_2 CYLINDER
θ
$4\frac{1}{4}$"
$1\frac{3}{4}$"
COUNTER #5c
COUNTER #5a
0 1 2
SCALE IN INCHES

FIG. 12

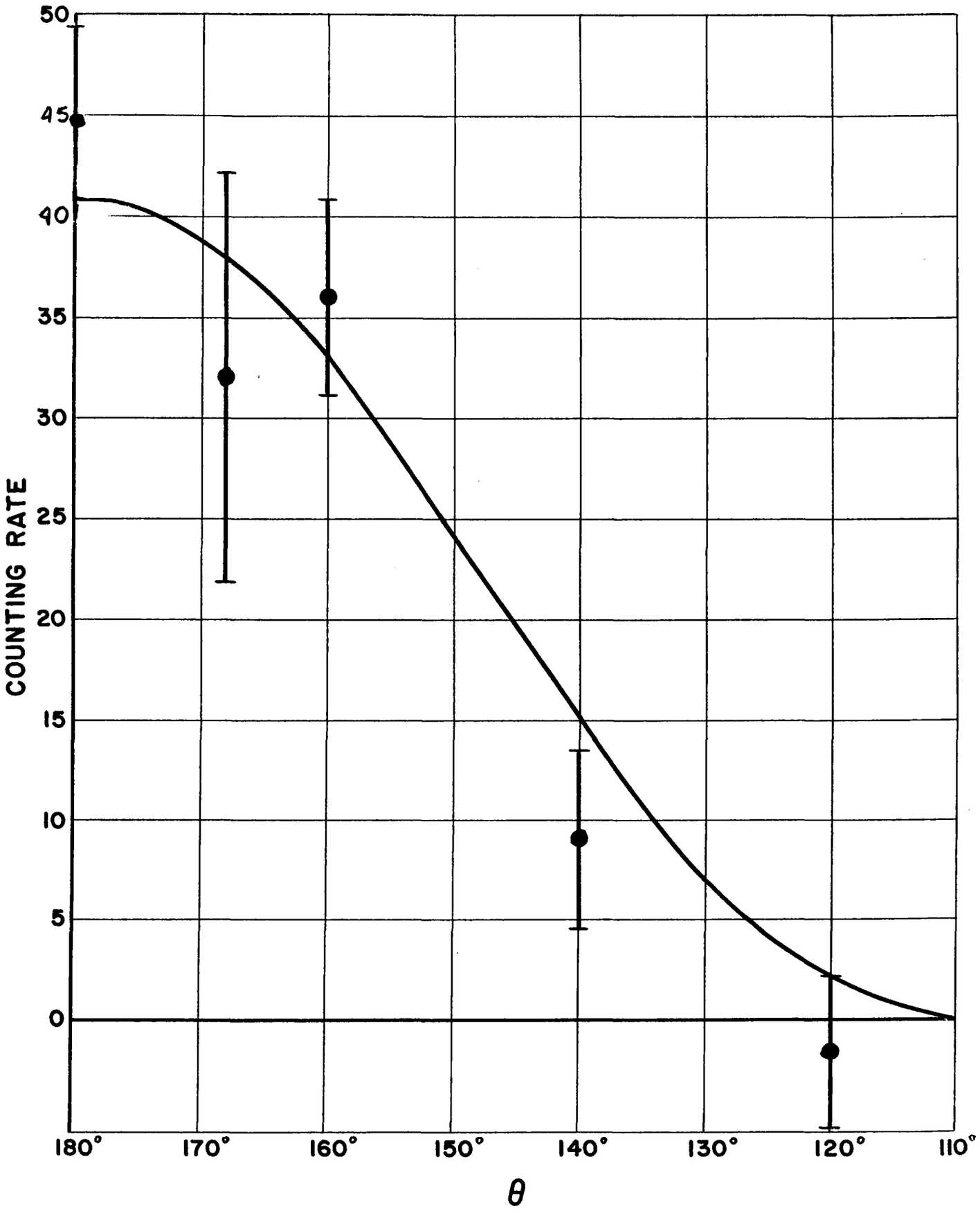
50
45
40
35
30
25
20
15
10
5
0
COUNTING RATE
180°
170°
160°
150°
140°
130°
120°
110°
θ

FIG. 13

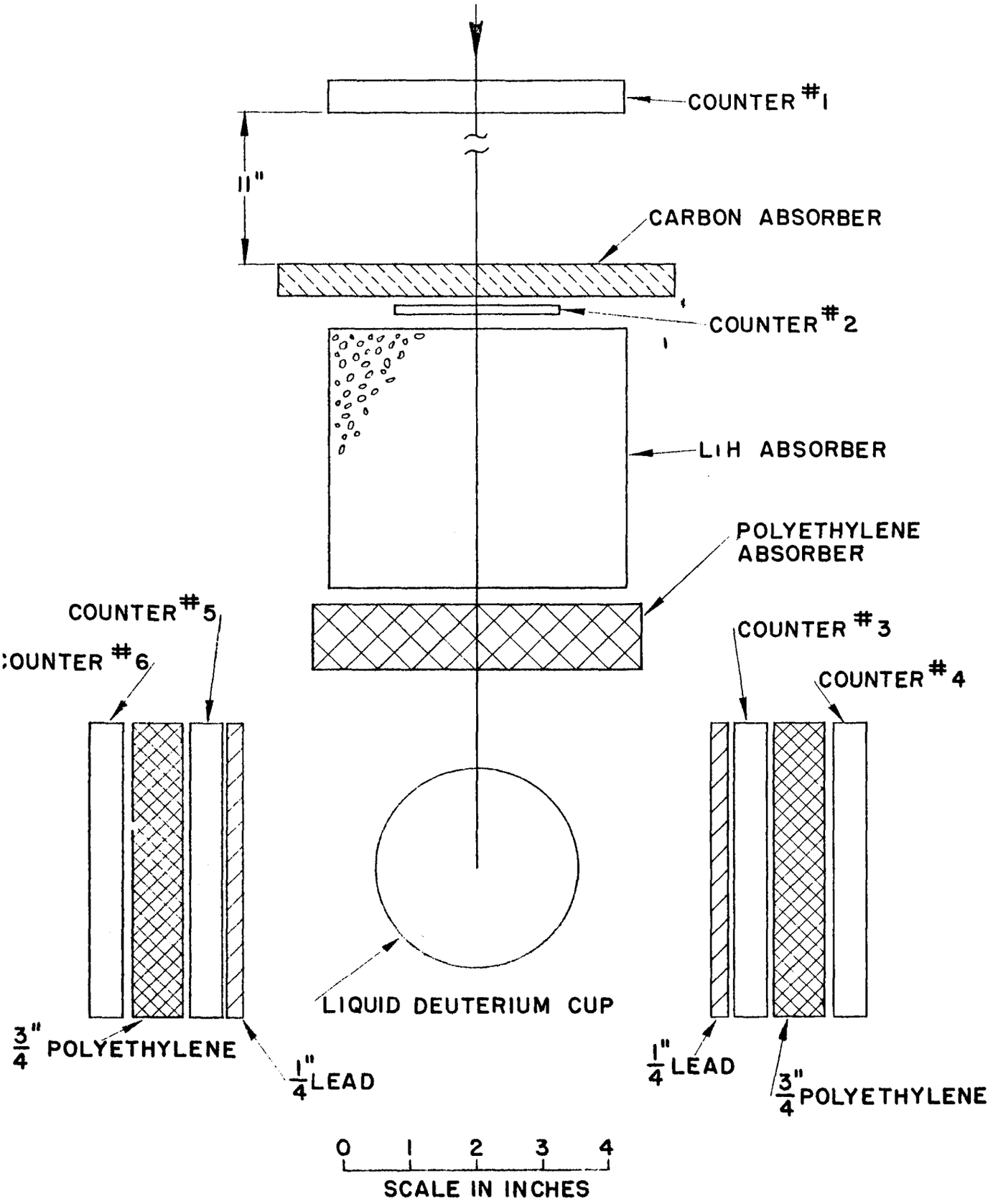
COUNTER #1
11"
CARBON ABSORBER
COUNTER #2
LiH ABSORBER
POLYETHYLENE ABSORBER
COUNTER #5
COUNTER #6
COUNTER #3
COUNTER #4
LIQUID DEUTERIUM CUP
3/4" POLYETHYLENE
1/4" LEAD
1/4" LEAD
3/4" POLYETHYLENE
0 1 2 3 4
SCALE IN INCHES

FIG. 14